Reduced-Order Modeling of Large Linear Passive Multi-terminal Circuits Using Matrix-Padé Approximation*

Roland W. Freund
Bell Laboratories
Lucent Technologies
Room 2C–420
700 Mountain Avenue
Murray Hill, NJ 07974–0636, USA

Peter Feldmann
Bell Laboratories
Lucent Technologies
Room 2C–217
700 Mountain Avenue
Murray Hill, NJ 07974–0636, USA

Abstract

This paper introduces SyMPVL, an algorithm for the computation of the symmetric multi-port transfer function of an RLC circuit. The algorithm employs a novel symmetric block-Lanczos algorithm to reduce the original circuit matrices to a pair of banded symmetric matrices. These matrices, which are typically much smaller than the circuit matrices, determine a reduced-order model of the original multi-port. The transfer function of the model represents a matrix-Padé approximation of the multi-port matrix transfer function. In this paper, we describe the symmetric formulation of RLC multi-port transfer functions, present the symmetric block-Lanczos algorithm, prove stability and passivity of the reduced-order models in the RL, RC, and LC special cases, and report numerical results for SyMPVL applied to example circuits.

1 Introduction

Electronic circuits often contain large linear subnetworks of passive components. Such subnetworks may represent interconnect automatically extracted from layout as large RLC networks, models of IC packages, models of wireless propagation channels, etc.

In general, we are interested only in the behavior of the linear subnetworks at their terminals. This behavior can be fully characterized by a matrix-valued transfer function.

*Numerical Analysis Manuscript No. 97–4–03, Bell Laboratories, Murray Hill, New Jersey, February 1997. Available on WWW at {http://cm.bell-labs.com/cs/doc/97}.

We will show in this paper that in most practical cases, a very closely approximating matrix-valued transfer function can be obtained from a model that is several orders of magnitude "smaller" than the original circuit.

In [7], we introduced MPVL (**M**atrix **P**adé **V**ia a **L**anczos-type process), an algorithm for the accurate and efficient computation of reduced-order models of large linear circuits. MPVL generates a reduced-order model, the transfer function of which represents the matrix-Padé approximation of the original circuit's matrix transfer function. MPVL is a general algorithm, in the sense that it can stably compute reduced-order models for any linear system, and for different number of inputs and outputs, up to the desired level of accuracy. In contrast, RLC circuits can be characterized in terms of square and symmetric matrix transfer functions. Moreover, all the matrices resulting from formulating the RLC circuit equations are symmetric. Direct application of the MPVL algorithm to RLC circuits does not take advantage of this special structure and cannot guarantee in general the preservation of stability and passivity of the approximation.

The preservation of the stability and passivity properties of the circuits they are modeling is a major requirement for reduced-order models. Obviously, RLC circuits, being composed entirely of passive components, are always stable and passive. This property should not be violated by the reduced-order models.

In this paper we introduce SyMPVL, an algorithm that computes symmetric matrix-Padé approximations of the circuit matrix transfer function, using a novel symmetric block-Lanczos algorithm. The algorithm also produces increasingly more accurate reduced-order models of the original circuit and, in the important special cases of RL, RC, and LC circuits, guarantees stability and passivity at any order of approximation. For the general case, while no guarantees can be made for arbitrary approximation orders, once the model is sufficiently accurate, stability and passivity of the reduced-order model can be enforced by simple post-processing. The work described in this present paper generalizes SyPVL [9], which is an algorithm for computing single-input single-output transfer functions and models.

Alternative approaches, not based on Padé approximation, for generating reduced-order models for RLC circuits, also exist. In [19], a block-Arnoldi algorithm is employed. Another approach is PACT, which relies on pole matching and is described in [13].

The remainder of the paper is organized as follows. In Section 2, we present the symmetric formulation of the general RLC circuit transfer functions together with the RL, RC, and LC special cases. Section 3 discusses the matrix-Padé approximation of circuit transfer functions. Section 4 introduces a novel symmetric block-Lanczos algorithm that is used to compute the matrix-Padé approximation. In Section 5, we discuss stability and passivity properties. In Section 6, we report the results of numerical experiments with SyMPVL.

2 Symmetric Formulation of Circuit Equations

In this section, we first formulate the equations that describe general RLC circuits, and then we discuss the special cases of RC, RL, and LC circuits. We show that the matrices associated with the circuit equations are always symmetric and, in the special cases, they are also positive semi-definite These properties are important for the SyMPVL algorithm and for stability and passivity proofs.

2.1 General RLC Circuits

The connectivity of a circuit can be captured using a directional graph. The nodes of the graph correspond to the nodes of the circuit, and the edges of the graph correspond to each of the circuit elements. An arbitrary direction is assigned to graph edges, so one can distinguish between the source and destination nodes. The adjacency matrix, $\mathbf{A}$, of the directional graph describes the connectivity of a circuit. Each row of the matrix corresponds to a graph edge and, therefore, to a circuit element. Each column of the matrix corresponds to a graph or circuit node. The column corresponding to the datum (ground) node of the circuit is omitted in order to remove redundancy. By convention, a row of the connectivity matrix will contain $+1$ in the column corresponding to the source node, -1 in the column corresponding to the destination node, and 0 everywhere else. It is easy to see that Kirchhoff's laws, which depend only on connectivity can be expressed using the adjacency matrix

$$\begin{aligned} \text{KCL:} \quad & \mathbf{A}^{\mathrm{T}}\mathbf{i}_b = 0, \\ \text{KVL:} \quad & \mathbf{A}\mathbf{v}_n = \mathbf{v}_b, \end{aligned} \tag{1}$$

where $\mathbf{i}_b$ and $\mathbf{v}_b$ are the vectors of branch currents and voltages, respectively, and $\mathbf{v}_n$ is the vector of the non-datum node voltages.

We are interested in analyzing RLC circuits and for simplicity we assume that the circuit is excited just by current sources. In this case the adjacency matrix and the branch current and voltage vectors can be partitioned according to circuit-element types as follows:

$$\mathbf{A} = \begin{bmatrix} \mathbf{A}_i \\ \mathbf{A}_g \\ \mathbf{A}_c \\ \mathbf{A}_l \end{bmatrix}, \quad \mathbf{v}_b = \begin{bmatrix} \mathbf{v}_i \\ \mathbf{v}_g \\ \mathbf{v}_c \\ \mathbf{v}_l \end{bmatrix}, \quad \mathbf{i}_b = \begin{bmatrix} \mathbf{i}_i \\ \mathbf{i}_g \\ \mathbf{i}_c \\ \mathbf{i}_l \end{bmatrix}. \tag{2}$$

Here, the subscripts i, g, c, and l stand for branches containing current sources, resistors, capacitors, and inductors, respectively.

The set of circuit equations is completed by adding the so-called *branch constitutive relationships* (BCR's), which describe the physical behavior of the circuit elements. In the case of RLC circuits, the BCR's are as follows:

$$\mathbf{i}_i = -\mathbf{I}_t(t), \quad \mathbf{i}_g = \mathcal{G}\mathbf{v}_G, \quad \mathbf{i}_c = \mathcal{C}\frac{d}{dt}\mathbf{v}_c, \quad \mathbf{v}_l = \mathcal{L}\frac{d}{dt}\mathbf{i}_L. \tag{3}$$

Here, $\mathbf{I}_t(t)$ is the vector of current-source values, $\mathcal{G}$ and $\mathcal{C}$ are appropriately-sized diagonal matrices whose diagonal entries are the conductance and capacitance values of each element. It is clear that these values are positive for any physical circuit. The matrix $\mathcal{L}$ is also diagonal in the absence of inductive coupling. Inductive coupling introduces off-diagonal terms in the inductance matrix, but $\mathcal{L}$ remains symmetric and positive definite.

The modified nodal formulation (MNA) of the circuit equations is obtained by combining the Kirchhoff equations (1) with the BCRs (3), and eliminating as many current unknowns as possible. For the case of RLC circuits only inductor currents need to be left as unknowns. The resulting MNA equations are as follows:

$$\begin{aligned} \mathbf{A}_g^{\mathrm{T}}\mathcal{G}\mathbf{A}_g\mathbf{v}_n + \mathbf{A}_c^{\mathrm{T}}\mathcal{C}\mathbf{A}_c\tfrac{d}{dt}\mathbf{v}_n + \mathbf{A}_l^{\mathrm{T}}\mathbf{i}_L &= A_i^{\mathrm{T}}\mathbf{I}_t(t), \\ \mathbf{A}_l\mathbf{v}_n - \mathcal{L}\frac{d}{dt}\mathbf{i}_L &= 0. \end{aligned} \tag{4}$$

Writing (4) in matrix form, we obtain

$$\underbrace{\begin{bmatrix} \mathbf{A}_g^{\mathrm{T}}\mathcal{G}\mathbf{A}_g & \mathbf{A}_l^{\mathrm{T}} \\ \mathbf{A}_l & 0 \end{bmatrix}}_{\mathbf{G}} \underbrace{\begin{bmatrix} \mathbf{v}_n \\ \mathbf{i}_l \end{bmatrix}}_{\mathbf{x}} + \underbrace{\begin{bmatrix} \mathbf{A}_c^{\mathrm{T}}\mathcal{C}\mathbf{A}_c & 0 \\ 0 & -\mathcal{L} \end{bmatrix}}_{\mathbf{C}} \underbrace{\frac{d}{dt}\begin{bmatrix} \mathbf{v}_n \\ \mathbf{i}_L \end{bmatrix}}_{\frac{d}{dt}\mathbf{x}} = \underbrace{\begin{bmatrix} \mathbf{A}_i^{\mathrm{T}} \\ 0 \end{bmatrix}}_{\mathbf{B}} \mathbf{I}_l(t). \tag{5}$$

Note that the matrices $\mathbf{G}$ and $\mathbf{C}$ are symmetric. They are however indefinite in general.

We are interested in determining the network functions of the RLC block viewed as a p-terminal component. Since we allowed only current sources in our formulation, it is natural to determine the Z-parameters. By applying the Laplace transform and assuming zero initial conditions, we obtain

$$\begin{aligned} (\mathbf{G} + s\mathbf{C})\mathbf{X} &= \mathbf{B}\,\mathbf{I}_s(s), \\ \mathbf{V}_i &= \mathbf{B}^{\mathrm{T}}\mathbf{X}. \end{aligned} \tag{6}$$

Here, $\mathbf{X}$, $\mathbf{I}_s(s)$, and $\mathbf{V}_i$ represent the Laplace transforms of the unknown vector $\mathbf{x}$, the excitation current $\mathbf{I}_l(t)$, and the vector of voltages across the excitation sources, respectively. Eliminating $\mathbf{X}$ in (6) gives

$$\mathbf{V}_i = \begin{bmatrix} \mathbf{A}_i & 0 \end{bmatrix} \mathbf{X} = \underbrace{\mathbf{B}^{\mathrm{T}}(\mathbf{G} + s\mathbf{C})^{-1}\mathbf{B}}_{\mathbf{Z}(s)} \mathbf{I}_s(s). \tag{7}$$

While for general RLC circuits the matrices $\mathbf{G}$ and $\mathbf{C}$ are indefinite, in some important special cases the formulation can be modified such that the matrices become positive semi-definite. In these special cases, important passivity and stability results can be proven.

2.2 Special Cases: RC, RL, LC Circuits

In the case of RC circuits, the matrices $\mathcal{L}$, $\mathbf{A}_l$, and the vector $\mathbf{i}_l$ are empty. The Laplace transform of the MNA equations (4) thus reduces to

$$\underbrace{\mathbf{A}_g^{\mathrm{T}}\mathcal{G}A_g}_{\mathbf{G}} \mathbf{V}_n + \underbrace{\mathbf{A}_c^{\mathrm{T}}\mathcal{C}\mathbf{A}_c}_{\mathbf{C}} s\mathbf{V}_n = \mathbf{A}_i^{\mathrm{T}}\mathbf{I}_s(s). \tag{8}$$

Clearly, the matrices $\mathbf{C}$ and $\mathbf{G}$ are symmetric positive semi-definite.

In the case of RL circuits, the matrices $\mathcal{C}$ and $\mathbf{A}_c$ are empty. The Laplace transform of the MNA equations (4) now becomes

$$\begin{aligned} \mathbf{A}_g^{\mathrm{T}}\mathcal{G}\mathbf{A}_g\mathbf{V}_n + \mathbf{A}_l^{\mathrm{T}}\mathbf{I}_l &= \mathbf{A}_i^{\mathrm{T}}\mathbf{I}_s(s), \\ \mathbf{A}_l\mathbf{V}_n - \mathcal{L}s\mathbf{I}_l &= 0. \end{aligned} \tag{9}$$

By multiplying the first equation in (9) by s and substituting $s\mathbf{I}_l$ from the second, we obtain

$$\underbrace{\mathbf{A}_g^{\mathrm{T}}\mathcal{G}\mathbf{A}_g}_{\mathbf{C}} \mathbf{V}_n s + \underbrace{\mathbf{A}_l^{\mathrm{T}}\mathcal{L}^{-1}\mathbf{A}_l}_{\mathbf{G}} \mathbf{V}_n = s\mathbf{A}_i^{\mathrm{T}}\mathbf{I}_s(s), \tag{10}$$

where the matrices $\mathbf{C}$ and $\mathbf{G}$ are again symmetric positive semi-definite.

In the case of LC circuits, the matrices $\mathcal{G}$ and $\mathbf{A}_g$ are empty. The Laplace transform of the MNA equations (4) reduced to

$$\begin{aligned} \mathbf{A}_c^{\mathrm{T}} \mathcal{C} \mathbf{A}_c s \mathbf{V}_n + \mathbf{A}_l^{\mathrm{T}} \mathbf{I}_l &= \mathbf{A}_i^{\mathrm{T}} \mathbf{I}_s(s), \\ \mathbf{A}_l \mathbf{V}_n - \mathcal{L} s \mathbf{I}_l &= 0. \end{aligned} \tag{11}$$

By multiplying the first equation in (11) by s and substituting sI_L from the second, we obtain

$$\underbrace{\mathbf{A}_c^{\mathrm{T}} \mathcal{C} \mathbf{A}_c}_{\mathbf{C}} \mathbf{V}_n s^2 + \underbrace{\mathbf{A}_l^{\mathrm{T}} \mathcal{L}^{-1} \mathbf{A}_l}_{\mathbf{G}} = s \mathbf{A}_i^{\mathrm{T}} \mathbf{I}_s(s). \tag{12}$$

Again, the matrices $\mathbf{C}$ and $\mathbf{G}$ are symmetric positive semi-definite and a change of variables $\sigma = s^2$ brings 12 to the usual form.

3 Padé Approximation of Matrix Transfer Functions

Recall from (7) that the transfer function of an p-port is of the form

$$\mathbf{Z}(s) = \mathbf{B}^{\mathrm{T}} (\mathbf{G} + s\mathbf{C})^{-1} \mathbf{B}, \quad s \in \mathbb{C}, \tag{13}$$

where $\mathbf{G}$ and $\mathbf{C}$ are real symmetric $N \times N$ matrices, and $\mathbf{B}$ is a real $N \times p$ matrix. Note that $\mathbf{Z}$ is a matrix-valued rational function:

$$\mathbf{Z} \,:\, \mathbb{C} \longmapsto (\mathbb{C} \cup \{\infty\})^{p \times p}. \tag{14}$$

Moreover, each pole s of $\mathbf{Z}$ is also an eigenvalue of the matrix pencil $\mathbf{G} + \lambda \mathbf{C}$, i.e., each pole s of $\mathbf{Z}$ satisfies the equation $\det(\mathbf{G} + s\mathbf{C}) = 0$.

3.1 Review of the Case $p = 1$

For the moment, assume that $p = 1$. In this case, $\mathbf{Z}$ is a scalar-valued rational function, and for each n, we can define a scalar-valued Padé approximant $\mathbf{Z}_n$ to $\mathbf{Z}$ as follows. A function of the form

$$\mathbf{Z}_n(s) = \frac{\phi_{n-1}(s)}{\psi_n(s)}, \tag{15}$$

where ϕ_{n-1} and ψ_n are polynomials of degree at most $n-1$ and n, respectively, is called an nth *Padé approximant* to $\mathbf{Z}$ if

$$\mathbf{Z}(s) = \mathbf{Z}_n(s) + \mathcal{O}(s^{q(n)}), \tag{16}$$

where $q(n)$ is as large as possible; see, e.g., [3]. The condition (16) means that the Taylor expansions of $\mathbf{Z}$ and $\mathbf{Z}_n$ about $s = 0$ agree in as many leading Taylor coefficients (the so-called *moments*) as possible. In general, $q(n) = 2n$.

The standard approach to computing $\mathbf{Z}_n$ is based on explicit moment generation. First, one computes the leading $q(n)$ Taylor coefficients of $\mathbf{Z}$, and from these, one then generates the coefficients of the polynomials ϕ_{n-1} and ψ_n in (15). This standard approach to computing $\mathbf{Z}_n$ is employed in the asymptotic waveform evaluation (AWE) technique [15, 16]. However, computing Padé approximants using explicit moment computations is inherently numerically unstable, and indeed, in practice, this approach can be used only for very moderate values of n, such as $n \leq 10$; see [6]. These numerical instabilities can be avoided by exploiting the Lanczos-Padé connection [12] and generating the Padé approximant $\mathbf{Z}_n$ via the Lanczos process [14]. The resulting algorithms for stably computing Padé approximants of transfer function are PVL [5, 6] for general circuits and its special variant SyPVL [9] for RLC circuits. In SyPVL, the Padé approximant $\mathbf{Z}_n$ is computed using the formula

$$\mathbf{Z}_n(s) = \boldsymbol{\rho}_n^{\mathrm{T}} \left(\mathbf{A}_n + s\mathbf{B}_n\right)^{-1} \boldsymbol{\rho}_n, \tag{17}$$

where the $n \times n$ matrices $\mathbf{A}_n$, $\mathbf{B}_n$ and the vector $\boldsymbol{\rho}_n$ are generated from a symmetric version of the Lanczos process.

3.2 The General Case $p \geq 1$

Now we return to the general case of p-ports with $p \geq 1$. One approach to obtaining approximations of $\mathbf{Z}$ is to compute scalar Padé approximants for each of the p^2 entries of $\mathbf{Z}$ by means of p^2 runs of PVL. However, a much more efficient approach is to use the concept of matrix-Padé approximation [3] that generates a matrix-valued approximation $\mathbf{Z}_n$ for all entries of $\mathbf{Z}$ in one run. Moreover, the reduced-order model generated by $\mathbf{Z}_n$ is much smaller than the reduced-order model obtained from p^2 individual PVL runs.

In analogy to (15), matrix-Padé approximants can be represented by means of a pair of numerator and denominator matrix polynomials whose coefficients can be obtained via explicit moment computations. However, this approach suffers from the same instability mentioned above for the case $p = 1$. Instead, we use an appropriate extension of the formula (17) to the general matrix case $p \geq 1$ in our definition of matrix-Padé approximants. More precisely, we say that a matrix-valued function

$$\mathbf{Z}_n \,:\, \mathbb{C} \longmapsto (\mathbb{C} \cup \{\infty\})^{p \times p}. \tag{18}$$

is an nth *matrix-Padé approximant* to $\mathbf{Z}$ if $\mathbf{Z}_n$ is of the form

$$\mathbf{Z}_n(s) = \boldsymbol{\rho}_n^{\mathrm{T}} \left(\mathbf{A}_n + s\mathbf{B}_n\right)^{-1} \boldsymbol{\rho}_n, \quad \text{where } \boldsymbol{\rho}_n \in \mathbb{C}^{n \times p} \text{ and } \mathbf{A}_n,\, \mathbf{B}_n \in \mathbb{C}^{n \times n} \tag{19}$$

and

$$\mathbf{Z}(s) = \mathbf{Z}_n(s) + \mathcal{O}(s^{q(n)}) \quad \text{with maximal } q(n). \tag{20}$$

In general, we have $q(n) \geq 2\lfloor n/p \rfloor$, with $q(n) > 2\lfloor n/p \rfloor$ if, and only if, so-called *deflation* occurs due to certain linear dependencies.

In the next section, we formulate a symmetric Lanczos-type algorithm that generates appropriate matrices $\mathbf{A}_n$, $\mathbf{B}_n$, and $\boldsymbol{\rho}_n$ such that the function $\mathbf{Z}_n$ defined in (19) is indeed an nth matrix-Padé approximant to $\mathbf{Z}$.

4 A Symmetric Lanczos-Type Algorithm

In order to compute matrix-Padé approximants to matrix-valued transfer functions (13), we need a Lanczos-type algorithm that can handle multiple starting vectors, namely the p columns of the matrix $\mathbf{B}$ in (13). Such a procedure was recently developed in [1] and further refined in [8]. We use a special symmetric variant of the algorithm described in [8] that exploits the symmetry of the matrices $\mathbf{G}$ and $\mathbf{C}$ in (13). We stress that Lanczos-type algorithms for multiple starting vectors are necessarily quite involved for two reasons. First, in the course of the algorithm, some of the generated vectors can become linearly dependent and thus need to be *deflated*. Second, so-called *look-ahead* techniques are required to avoid potential breakdowns due to division by quantities that cannot be excluded to be zero. The algorithm used here is the only existing Lanczos-type process that has both deflation and look-ahead built in.

Next, we give a precise statement of the symmetric Lanczos-type procedure used to compute matrix-Padé approximants to $\mathbf{Z}$. This algorithm could be directly stated in terms of $\mathbf{G}$, $\mathbf{C}$, and $\mathbf{B}$, but then we would have to either store additional vectors or to abandon the modified Gram-Schmidt orthogonalization used within the algorithm. Instead, we assume that $\mathbf{G}$ is factored as

$$\mathbf{G} = \mathbf{M}\,\mathbf{J}\,\mathbf{M}^{\mathrm{T}}, \quad \text{where} \quad \mathbf{M},\ \mathbf{J} \in \mathbb{R}^{N\times N}, \tag{21}$$

and $\mathbf{J}$ is a "simple" matrix, such as, e.g., a diagonal matrix. For example, if $\mathbf{M}$ is real symmetric positive definite, then we can choose $\mathbf{J} = \mathbf{I}$ (the $N \times N$ identity matrix). A factorization (21) can be computed via a suitable version of the Bunch-Parlett-Kaufman algorithm if $\mathbf{G}$ is indefinite, or a version of the Cholesky algorithm if $\mathbf{G}$ is symmetric positive definite; see, e.g., [11]. We now state the Lanczos-type algorithm in terms of $\mathbf{M}$, $\mathbf{M}^{\mathrm{T}}$, $\mathbf{J}$, $\mathbf{C}$, and $\mathbf{B}$. This corresponds to rewriting the transfer function (13) as

$$\mathbf{Z}(s) = \left(\mathbf{M}^{-1}\mathbf{B}\right)^{\mathrm{T}} \left(\mathbf{J} + s\mathbf{M}^{-1}\mathbf{C}\,\mathbf{M}^{-\mathrm{T}}\right)^{-1} \left(\mathbf{M}^{-1}\mathbf{B}\right), \tag{22}$$

and applying the Lanczos procedure to the matrix

$$\mathbf{A} = \mathbf{M}^{-1}\mathbf{C}\,\mathbf{M}^{-\mathrm{T}} \tag{23}$$

with starting vectors $\mathbf{M}^{-1}\mathbf{B}$, and constructing the Lanczos vectors $\mathbf{v}_1, \mathbf{v}_2, \ldots$, to be $\mathbf{J}$-orthogonal. More precisely, if no look-ahead steps are necessary, the Lanczos vectors satisfy

$$\mathbf{v}_i^{\mathrm{T}}\,\mathbf{J}\,\mathbf{v}_n = \begin{cases} \delta_n & \text{if } i = n, \\ 0 & \text{if } i \neq n, \end{cases} \qquad \text{for all} \quad i, n = 1, 2, \ldots . \tag{24}$$

If look-ahead steps do occur, then the Lanczos vectors are only cluster-wise $\mathbf{J}$-orthogonal, instead of the vector-wise $\mathbf{J}$-orthogonality (24).

We note that after n steps of the Lanczos-type algorithm below, the Lanczos vectors

$$\mathbf{v}_1, \mathbf{v}_2, \ldots, \mathbf{v}_n \tag{25}$$

have been constructed. In addition, at the end of each nth step, there are $p_c = p_c(n)$ "auxiliary" vectors,

$$\hat{\mathbf{v}}_{n+1}, \hat{\mathbf{v}}_{n+2}, \ldots, \hat{\mathbf{v}}_{p_c}, \tag{26}$$

available. These vectors will be turned into Lanczos vectors or deflated in successive iterations. Here, p_c denotes the current block size. Initially, $p_c = p$, and then within the algorithm p_c is reduced by one every time a deflation occurs.

Algorithm 1 (Symmetric Lanczos-type method with deflation and look-ahead.)
INPUT: Matrices $\mathbf{G} = \mathbf{G}^{\mathrm{T}} = \mathbf{M}\,\mathbf{J}\,\mathbf{M}^{\mathrm{T}}$, $\mathbf{C} = \mathbf{C}^{\mathrm{T}} \in \mathbb{R}^{N\times N}$;
A block $\mathbf{B} = \begin{bmatrix}\mathbf{b}_1 & \mathbf{b}_2 & \cdots & \mathbf{b}_p\end{bmatrix} \in \mathbb{R}^{N\times p}$ of p starting vectors (the vectors $\mathbf{b}_i$).
OUTPUT: An $p_1 \times p$ matrix $\boldsymbol{\rho}$;
($p_1 = p -$(# of deflations during the first p iterations).)
The nonzero entries of the $n \times n$ matrices $\mathbf{T}_n$ and $\boldsymbol{\Delta}_n$.
(Here, n is the value of the iteration counter at termination.)

0) *For* $i = 1, 2, \ldots, p$, *set*

$$\hat{\mathbf{v}}_i = \mathbf{J}^{-1}\mathbf{M}^{-1}\mathbf{b}_i.$$

Set $p_c = p$.
(p_c is the current block size.)
Set $\mathcal{I}_{\mathbf{v}} = \emptyset$.
($\mathcal{I}_{\mathbf{v}}$ records indices of clusters that must be preserved due to inexact deflation. If $k \in \mathcal{I}_{\mathbf{v}}$, then the newly constructed $\mathbf{v}$ vectors need to be $\mathbf{J}$-orthogonalized against all vectors $\mathbf{v}_i$ with $i \in \mathcal{C}_k$.)
Set $\gamma = 1$, $\mathcal{C}_\gamma = \emptyset$, *and* $\mathbf{V}^{(\gamma)} = \emptyset$.
(γ is the number of the currently constructed look-ahead cluster, and $\mathcal{C}_\gamma$ is the set of indices of the already constructed Lanczos vectors in the γth cluster $\mathbf{V}^{(\gamma)}$.)

For $n = 1, 2, \ldots,$ *do* (Build nth Lanczos vector $\mathbf{v}_n$.) :

1) (Perform deflation (if necessary) and obtain $\mathbf{v}_n$.)

1a) (Decide if $\hat{\mathbf{v}}_n$ should be deflated.)

(i) *Set* $\phi = n - p_c$.

(ii) *If the current* γ*th cluster contains at least one vector, i.e.,* $\mathcal{C}_\gamma \neq \emptyset$, *then orthogonalize* $\hat{\mathbf{v}}_n$ *against the vectors* $\mathbf{v}_i$ *in that cluster*:
For all $i \in \mathcal{C}_\gamma$ (*in ascending order*), *set*

$$\tau_{i,\phi} = \frac{\mathbf{v}_i^{\mathrm{H}}\hat{\mathbf{v}}_n}{\|\mathbf{v}_i\|^2}, \quad \hat{\mathbf{v}}_n = \hat{\mathbf{v}}_n - \mathbf{v}_i\tau_{i,\phi}, \quad \textit{and} \quad t_{i,\phi} = t_{i,\phi} + \tau_{i,\phi}.$$

(iii) (Deflate if $\|\hat{\mathbf{v}}_n\|$ is "small".)
If $\|\hat{\mathbf{v}}_n\| >$ `dtol`, *then continue with step* 1b).
Otherwise, deflate $\hat{\mathbf{v}}_n$ *by doing the following* :

(iv) *If* $p_c = 1$, *then stop.*
(There are no more Krylov vectors.)

(v) *If* $\phi > 0$ *and the deflated vector* $\hat{\mathbf{v}}_n$ *is nonzero, then set* $\mathcal{I}_{\mathbf{v}} = \mathcal{I}_{\mathbf{v}} \cup \{\, \gamma(\phi) \,\}$, *and save the vectors* $\mathbf{v}_i$, $i \in \mathcal{C}_{\gamma(\phi)}$.

(vi) *Set* $p_{\mathrm{c}} = p_{\mathrm{c}} - 1$.
(The current block size is reduced by one.)

(vii) *For* $i = n, n+1, \ldots, n+p_{\mathrm{c}}-1$, *set* $\hat{\mathbf{v}}_i = \hat{\mathbf{v}}_{i+1}$.
(The auxiliary vector $\hat{\mathbf{v}}_n$ is deflated. The indices of the remaining auxiliary vectors are reduced by one.)

(vii) *Repeat step* 1a).

1b) (Normalize $\hat{\mathbf{v}}_n$ to obtain the nth Lanczos vector $\mathbf{v}_n$.)
Set

$$\mathbf{v}_n = \frac{\hat{\mathbf{v}}_n}{t_{n,n-p_{\mathrm{c}}}},$$

where $t_{n,n-p_{\mathrm{c}}}$ *is a suitable scaling factor, e.g.,*

$$t_{n,n-p_{\mathrm{c}}} = \|\hat{\mathbf{v}}_n\|_2 \,.$$

If $n \leq p_{\mathrm{c}}$, *then set* $\rho_{n,n-p_{\mathrm{c}}+m} = t_{n,n-p_{\mathrm{c}}}$.

1c) (Update cluster information.)
Set $\mathbf{V}^{(\gamma)} = \begin{bmatrix} \mathbf{V}^{(\gamma)} & \mathbf{v}_n \end{bmatrix}$, $\mathcal{C}_\gamma = \mathcal{C}_\gamma \cup \{n\}$, *and* $\gamma(n) = \gamma$.
($\gamma(n)$ is the index of the cluster containing the nth Lanczos vector $\mathbf{v}_n$.)
If $\mathcal{C}_\gamma = \{n\}$, *set* $\gamma_{\mathbf{v}} = \gamma\,(\max\{1, n-p_{\mathrm{c}}\})$.

2) (Compute $\boldsymbol{\Delta}^{(\gamma)}$ and check for end of look-ahead cluster.)

2a) *Form*

$$\boldsymbol{\Delta}^{(\gamma)} = \left(\mathbf{V}^{(\gamma)}\right)^{\mathrm{T}} \mathbf{J}\, \mathbf{V}^{(\gamma)}.$$

2b) (Decide if the current cluster is complete.)
If the matrix $\boldsymbol{\Delta}^{(\gamma)}$ *is singular (or in some sense "close" to singular), then continue with step* 3).
Otherwise, the current cluster is complete and the following "end-of-cluster" updates are performed :

2c) (**J**-orthogonalize the vectors $\hat{\mathbf{v}}_i$, $n+1 \leq i \leq n+p_{\mathrm{c}}-1$, against the vectors $\mathbf{v}_j$ in the current cluster.)
For $i = n+1, n+2, \ldots, n+p_{\mathrm{c}}-1$, *set*

$$\begin{aligned} \left[t_{j,i-p_{\mathrm{c}}}\right]_{j\in\mathcal{C}_\gamma} &= \left(\boldsymbol{\Delta}^{(\gamma)}\right)^{-1} \left(\mathbf{V}^{(\gamma)}\right)^{\mathrm{T}} \mathbf{J}\, \hat{\mathbf{v}}_i, \\ \hat{\mathbf{v}}_i &= \hat{\mathbf{v}}_i - \mathbf{V}^{(\gamma)} \left[t_{j,i-p_{\mathrm{c}}}\right]_{j\in\mathcal{C}_\gamma}, \end{aligned}$$

and if $i \leq p_{\mathrm{c}}$, *set* $\left[\rho_{j,i-p_{\mathrm{c}}+m}\right]_{j\in\mathcal{C}_\gamma} = \left[t_{j,i-p_{\mathrm{c}}}\right]_{j\in\mathcal{C}_\gamma}$.

2d) *Increment the cluster counter* $\gamma = \gamma + 1$;
Set $\gamma(n+1) = \gamma$, $\mathcal{C}_\gamma = \emptyset$, *and* $\mathbf{V}^{(\gamma)} = \emptyset$.
(The current cluster is complete, and so the vector $\mathbf{v}_{n+1}$ constructed in the next iteration will start a new cluster.)

3) (Advance the block Krylov subspace and obtain new vector $\hat{\mathbf{v}}_{n+p_c}$.)

3a) *Obtain*

$$\mathbf{v} = \mathbf{J}^{-1}\mathbf{M}^{-1}\mathbf{C}\,\mathbf{M}^{-\mathrm{T}}\,\mathbf{v}_n$$

by first solving the linear system

$$\mathbf{M}^{\mathrm{T}}\,\mathbf{t} = \mathbf{v}_n$$

for $\mathbf{t}$*, then solving the linear system*

$$\mathbf{M}\,\mathbf{v} = \mathbf{C}\,\mathbf{t}$$

for $\mathbf{v}$*, and finally setting* $\mathbf{v} = \mathbf{J}^{-1}\mathbf{v}$.

3b) ($\mathbf{J}$-orthogonalize $\mathbf{v}$ against previous Lanczos vectors.)

(i) ($\mathbf{J}$-orthogonalize $\mathbf{v}$ against clusters $\mathbf{V}^{(k)}$, $\gamma_{\mathbf{v}} \le k \le \gamma - 2$.)
Set

$$\boldsymbol{\delta} = \boldsymbol{\Delta}^{(\gamma-1)} \begin{bmatrix} 0 \\ \vdots \\ 0 \\ 1 \end{bmatrix}.$$

($\boldsymbol{\delta}$ is the last column of $\boldsymbol{\Delta}^{(\gamma-1)}$.)
For all $k = \gamma_{\mathbf{v}}, \gamma_{\mathbf{v}}+1, \ldots, \gamma-2$*, set*

$$\begin{aligned} \big[t_{j,n}\big]_{j\in\mathcal{C}_k} &= \big(\boldsymbol{\Delta}^{(k)}\big)^{-1} \Big(\big[t_{i,j}\big]_{i\in\mathcal{C}_{\gamma-1}, j\in\mathcal{C}_k}\Big)^{\mathrm{T}} \boldsymbol{\delta}, \\ \mathbf{v} &= \mathbf{v} - \mathbf{V}^{(k)}\big[t_{j,n}\big]_{j\in\mathcal{C}_k}. \end{aligned}$$

(ii) (Perform $\mathbf{J}$-orthogonalization of $\mathbf{v}$ due to inexact deflation.)
For all $k \in \mathcal{I}_{\mathbf{v}}$ *with* $k < \gamma_{\mathbf{v}}$ *(in ascending order), set*

$$\begin{aligned} \big[t_{j,n}\big]_{j\in\mathcal{C}_k} &= \big(\boldsymbol{\Delta}^{(k)}\big)^{-1} \big(\mathbf{V}^{(k)}\big)^{\mathrm{T}} \mathbf{J}\,\mathbf{v}, \\ \mathbf{v} &= \mathbf{v} - \mathbf{V}^{(k)}\big[t_{j,n}\big]_{j\in\mathcal{C}_k}. \end{aligned}$$

(iii) ($\mathbf{J}$-orthogonalize $\mathbf{v}$ against cluster $\mathbf{V}^{(\gamma-1)}$.)
Set

$$\begin{aligned} \big[t_{j,n}\big]_{j\in\mathcal{C}_{\gamma-1}} &= \big(\boldsymbol{\Delta}^{(\gamma-1)}\big)^{-1} \big(\mathbf{V}^{(\gamma-1)}\big)^{\mathrm{T}} \mathbf{J}\,\mathbf{v}, \\ \hat{\mathbf{v}}_{n+p_c} &= \mathbf{v} - \mathbf{V}^{(\gamma-1)}\big[t_{j,n}\big]_{j\in\mathcal{C}_{\gamma-1}}. \end{aligned}$$

To get the nth matrix-Padé approximant $\mathbf{Z}_n$ to $\mathbf{Z}$, we need the following quantities from Algorithm 1:

$$\begin{aligned} \boldsymbol{\rho} &= \big[\rho_{i,j}\big]_{1\le i\le p_1,\, 1\le j\le p}, \\ \mathbf{T}_n &= \big[t_{i,j}\big]_{1\le i\le n,\, 1\le j\le n}, \\ \boldsymbol{\Delta}_n &= \operatorname{diag}\Big(\boldsymbol{\Delta}^{(1)}, \boldsymbol{\Delta}^{(2)}, \ldots, \boldsymbol{\Delta}^{(\gamma)}\Big). \end{aligned} \tag{27}$$

Here, for $\boldsymbol{\rho}$ and $\mathbf{T}_n$ we use the convention that all the entries $\rho_{i,j}$ and $t_{i,j}$ that are not explicitly defined in Algorithm 1 are set to zero. Then

$$\mathbf{Z}_n(s) = \boldsymbol{\rho}_n^{\mathrm{T}} \left(\boldsymbol{\Delta}_n^{-1} + s\mathbf{T}_n\boldsymbol{\Delta}_n^{-1}\right)^{-1} \boldsymbol{\rho}_n, \quad \boldsymbol{\rho}_n = \begin{bmatrix} \boldsymbol{\rho} \\ \mathbf{0}_{n-p_1 \times p} \end{bmatrix}, \tag{28}$$

is the nth matrix-Padé approximant to $\mathbf{Z}$; see [8] for a rigorous proof of this statement. For later use, we remark that the matrix $\mathbf{T}_n$ can be viewed as a certain oblique projection of the matrix $\mathbf{A}$ defined in (23) onto the space spanned by the first n Lanczos vectors. More precisely, assuming for simplicity that only zero vectors $\hat{\mathbf{v}}_n = 0$ are deflated in Algorithm 1, we have

$$\mathbf{V}_n^{\mathrm{T}}\mathbf{J}\mathbf{A}\mathbf{V}_n = \boldsymbol{\Delta}_n\mathbf{T}_n, \tag{29}$$

where

$$\mathbf{V}_n = \begin{bmatrix} \mathbf{v}_1 & \mathbf{v}_2 & \cdots & \mathbf{v}_n \end{bmatrix}. \tag{30}$$

5 Stability and Passivity

For RLC circuits, Padé-based reduced-order models are in general not stable and not passive. However, if the order n is large enough so that the reduced-order models are sufficiently accurate, then the reduced-order models defined by $\mathbf{Z}_n$ are almost stable and passive, and can in fact be made stable and passive by a suitable "post-processing" of $\mathbf{Z}_n$. Such post-processing techniques will be described elsewhere.

In this section, we show that the reduced-order models defined by $\mathbf{Z}_n$ are guaranteed to be stable and passive for the special cases of RC, RL, and LC circuits.

5.1 Stability

Recall from the discussion in Section 2.2 that the matrices $\mathbf{G}$ and $\mathbf{C}$ in the formula (13) of the matrix transfer function $\mathbf{Z}$ are symmetric positive semi-definite for RC and RL circuits. Furthermore, for LC circuits, $\mathbf{Z}$ is given by (13) with s replaced by s^2, where $\mathbf{G}$ and $\mathbf{C}$ are again symmetric positive semi-definite.

Since $\mathbf{G}$ is symmetric positive semi-definite, it follows that $\mathbf{J} = \mathbf{I}$ in (21). As a result, the Lanczos vectors generated by Algorithm 1 are actually orthogonal, and thus $\boldsymbol{\Delta}_n = \mathbf{I}_n$ (the $n \times n$ identity matrix) for all n. Therefore, equation (28) reduces to

$$\mathbf{Z}_n(s) = \boldsymbol{\rho}_n^{\mathrm{T}} \left(\mathbf{I}_n + s\mathbf{T}_n\right)^{-1} \boldsymbol{\rho}_n. \tag{31}$$

Furthermore, the relation (29) now becomes

$$\mathbf{T}_n = \mathbf{V}_n^{\mathrm{T}}\mathbf{A}\mathbf{V}_n. \tag{32}$$

By (23), the matrix $\mathbf{A}$ has the same eigenvalues as the symmetric positive semi-definite matrix $\mathbf{C}$, and thus all eigenvalues of $\mathbf{A}$ are non-negative. Together with (32), it follows that $\mathbf{T}_n$ is symmetric positive semi-definite.

By (31), all poles of $\mathbf{Z}_n$ are of the form

$$s = -\frac{1}{\lambda}, \quad \text{where } \lambda \text{ is an eigenvalue of } \mathbf{T}_n. \tag{33}$$

Since $\mathbf{T}_n$ is symmetric positive semi-definite, $\lambda \geq 0$, and thus all poles of $\mathbf{Z}_n$ are non-positive. Moreover, it can be shown that a possible pole $s = 0$ is simple. Altogether, this proves that the reduced-order models defined by $\mathbf{Z}_n$ are stable for RC and RL circuits. The case of LC circuits can be handled similarly, using the formula (12) and the fact that the transformation $s \mapsto s^2$ maps the purely imaginary poles of an LC circuit into points on the negative real axis.

5.2 Passivity

We now show that the reduced-order models defined by $\mathbf{Z}_n$ are passive. Again, we only treat the case of RC and RL circuits, the case of LC circuits can be handled similarly after the transformation $s \mapsto s^2$ has been employed.

It is well known (see, e.g., [21, 2]) that the reduced-order model defined by the matrix-valued rational matrix $\mathbf{Z}_n$ given by (31) is passive if, and only if, the following three conditions are satisfied:

(i) $\mathbf{Z}_n(s)$ has no poles in $\{ s \in \mathbb{C} \mid \operatorname{Re} s > 0 \}$ (the right half of the complex plane);

(ii) $\mathbf{Z}_n(\bar{s}) = \overline{\mathbf{Z}_n(s)}$ for all $s \in \mathbb{C}$;

(iii) For all $s \in \mathbb{C}$ with $\operatorname{Re} s > 0$,

$$\operatorname{Re} \left(\mathbf{x}^{\mathrm{H}} \mathbf{Z}_n(s)\, \mathbf{x} \right) \geq 0 \quad \text{for all} \quad \mathbf{x} \in \mathbb{C}^p. \tag{34}$$

It thus remains to verify (i)–(iii). Condition (i) is satisfied in view of the stability of $\mathbf{Z}_n$. Condition (ii) follows immediately from (31) and the fact that $\mathbf{T}_n$ and $\boldsymbol{\rho}_n$ are are real matrices. Finally, we verify condition (iii). Let s be any complex number with $\operatorname{Re} s > 0$. Since $\mathbf{T}_n$ is symmetric positive semi-definite, we have

$$\operatorname{Re} \left(\mathbf{y}^{\mathrm{H}} \left(\mathbf{I} + \bar{s}\, \mathbf{T}_n \right) \mathbf{y} \right) = \|\mathbf{y}\|_2^2 + (\operatorname{Re} s) \mathbf{y}^{\mathrm{H}} \mathbf{T}_n \mathbf{y} \geq 0 \quad \text{for all} \quad \mathbf{y} \in \mathbb{C}^n. \tag{35}$$

For any given $\mathbf{x} \in \mathbb{C}^p$, we set

$$\mathbf{y} = \left(\mathbf{I} + s\, \mathbf{T}_n \right) \boldsymbol{\rho}_n \mathbf{x}. \tag{36}$$

Then $\mathbf{y} \in \mathbb{C}^n$, and inserting (36) into (35) gives

$$\begin{aligned} 0 \;&\leq \operatorname{Re} \left(\mathbf{y}^{\mathrm{H}} \left(\mathbf{I} + \bar{s}\, \mathbf{T}_n \right) \mathbf{y} \right) \\ &= \operatorname{Re} \left(\mathbf{x}^{\mathrm{H}} \boldsymbol{\rho}_n \left(\mathbf{I} + s \mathbf{T}_n \right)^{-1} \boldsymbol{\rho}_n \mathbf{x} \right) \\ &= \operatorname{Re} \left(\mathbf{x}^{\mathrm{H}} \mathbf{Z}_n(s)\, \mathbf{x} \right). \end{aligned} \tag{37}$$

Hence the reduced-order model given by $\mathbf{Z}_n$ is passive.

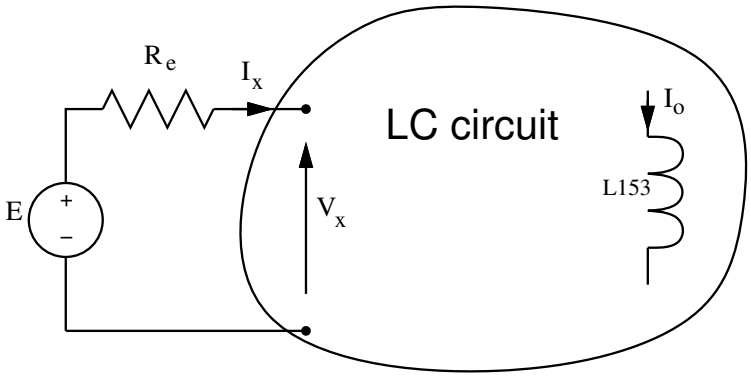

Figure 1: The PEEC circuit

6 Examples

In this section, we report numerical results for SyMPVL applied to two example circuits.

6.1 The PEEC Circuit

Our first example is the same circuit resulting from the PEEC modeling of an electromagnetic problem, which was used as example in [17]. The circuit consists of only inductors, capacitors, and inductive couplings and it is driven by a finite impedance source. We are interested in computing the response of this circuit, in this case the current flowing through one of the inductors.

The equations of the LC two-port are obtained by writing the KCL equations and differentiating them with respect to time gives

$$\mathbf{A}_l^{\mathrm{T}} s\mathbf{I}_l + \mathbf{A}_c^{\mathrm{T}} s\mathbf{I}_c + \mathbf{a} s\mathbf{I}_x = 0. \tag{38}$$

We substitute the inductor and capacitor equations

$$s\mathbf{I}_l = \mathcal{L}^{-1}\mathbf{V}_l = \mathcal{L}^{-1}\mathbf{A}_l\mathbf{V} \quad \text{and} \quad \mathbf{I}_c = \mathcal{C}s\mathbf{V}_c = \mathcal{C}\mathbf{A}_c s\mathbf{V} \tag{39}$$

into the differentiated KCL equation (38) and obtain the nodal circuit equations

$$\mathbf{A}_l^{\mathrm{T}}\mathcal{L}^{-1}\mathbf{A}_l V + \mathbf{A}_c^{\mathrm{T}}\mathcal{C}\mathbf{A}_c s^2\mathbf{V} + \mathbf{a} s\mathbf{I}_x = 0. \tag{40}$$

The output of interest is selected among the inductor currents, using the column vector $\mathbf{b}$. This results in the relation

$$s\mathbf{I}_o = \mathbf{b}^{\mathrm{T}} s\mathbf{I}_l = \underbrace{\mathbf{b}^{\mathrm{T}}\mathcal{L}^{-1}\mathbf{A}_l}_{\mathbf{l}^{\mathrm{T}}}\mathbf{V}. \tag{41}$$

Setting $\mathbf{G} = \mathbf{A}_l^{\mathrm{T}}\mathcal{L}^{-1}\mathbf{A}_l$ and $\mathbf{C} = \mathbf{A}_c^{\mathrm{T}}\mathcal{C}\mathbf{A}_c$, and simplifying s, the output of interest can be expressed as

$$I_o = \underbrace{-\mathbf{l}^{\mathrm{T}}(\mathbf{G} + s^2\mathbf{C})^{-1}\mathbf{a}}_{\alpha} \cdot I_x = \frac{\alpha}{R_e + Z_{in}} E. \tag{42}$$

The input impedance of the two-port is defined as the voltage V_x when a unit valued current is applied:

$$V_x = a^{\mathrm{T}}\mathbf{V} = \underbrace{-\mathbf{a}^{\mathrm{T}}(\mathbf{G}+s^2\mathbf{C})^{-1}\mathbf{a}s}_{Z_{in}} \cdot I_x. \tag{43}$$

The quantities needed to compute the response of the network are obtained from the two-by-two transfer matrix of the LC two-port

$$\mathbf{Z}(s) = \mathbf{B}^{\mathrm{T}}(\mathbf{G}+s^2\mathbf{C})^{-1}\mathbf{B}, \tag{44}$$

where $\mathbf{B}$ denotes the two-column matrix $\begin{bmatrix}\mathbf{a} & \mathbf{l}\end{bmatrix}$. Observe that

$$Z_{in} = -sh_{11}(s) \quad \text{and} \quad \alpha = -h_{21}(s). \tag{45}$$

The SyMPVL algorithm is applied to compute the matrix-Padé approximation of this two-by-two transfer function. In this case the matrix G is singular, or in electrical terms, there is no DC path to the reference voltage (ground) from every node. The transfer function computation requires therefore a frequency shift

$$\mathbf{Z}(s) = \mathbf{B}^{\mathrm{T}}\Big(\underbrace{\mathbf{G}+s_0\mathbf{C}}_{\hat{\mathbf{G}}} + \underbrace{(s^2-s_0)}_{\sigma}\mathbf{C}\Big)^{-1}\mathbf{B}. \tag{46}$$

In view of (28), the approximation will have the form

$$\mathbf{Z}_n(s) = \boldsymbol{\rho}_n^{\mathrm{T}}\left(\mathbf{I}+\sigma\mathbf{T}_n\right)^{-1}\boldsymbol{\rho}_n. \tag{47}$$

An approximation of order 50 was needed to obtain a good match of the function as illustrated in Figure 2. Since the change of variables included the square of s, we have in fact a matrix-Padé approximation of order $n = 50$, and we match $2\lfloor n/m \rfloor = 2\lfloor 50/2 \rfloor = 50$ matrix moments. Running the algorithm 6 more iterations results in a perfect match. Note that in this example the matrices $\mathbf{C}$ and $\mathbf{G}$ are real symmetric and positive definite, and therefore, the approximation always preserves all stability and passivity properties.

6.2 A Package Model

The next application is the analysis of a 64-pin package model used for an RF integrated circuit. Only eight of the package pins carry signal, the rest being either unused or necessary for supply voltages. The goal is to characterize the package as a 16-port component (8 exterior and 8 interior terminals) and apply SyMPVL model reduction on it. The reduced-order model can than replace the large package subcircuit in a circuit simulator resulting in considerable savings in simulation time.

The package model is described by approximatively 4000 circuit elements, resistors, capacitors, inductors, and inductive couplings. The size of the nodal circuit matrices for the package is about 2000.

Figures 3 and 4 show the voltage-to-voltage transfer function between the external terminal of pin no. 1 and the internal terminals of the same pin and the neighboring

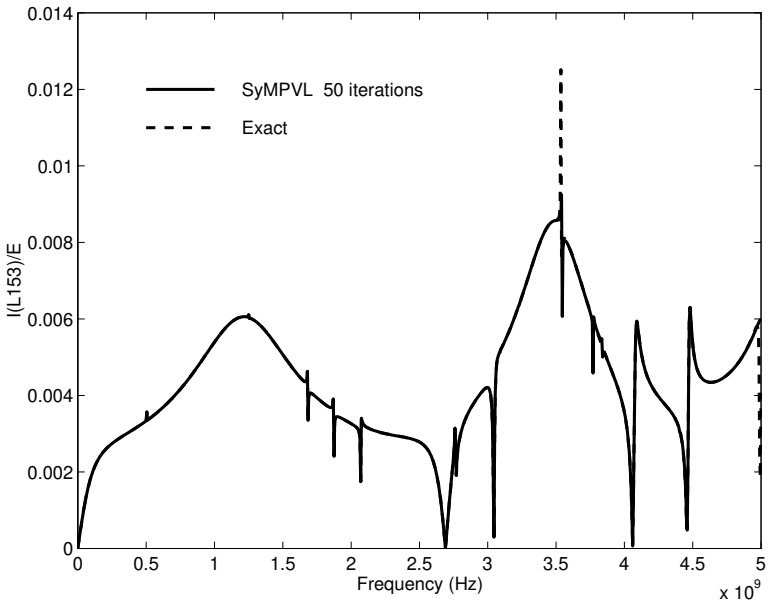

Figure 2: The PEEC circuit transfer function

pin no. 2, respectively. The plots show results with a reduced model of order 48, 64, and 80 compared with an exact analysis. The results show that reduced-order models can indeed replace the the full package subcircuit with little loss of accuracy. The reduction level depends on the desired accuracy. The most accurate of the models that gives an almost perfect match of the frequency response, only requires 80 state variables compared to 2000 for the full subcircuit. Since the cost of nonlinear circuit simulation is superlinear in the number of state variables the computational savings can be significant.

7 Concluding Remarks

In this paper, we have introduced SyMPVL as a tool to compute reduced-order models (based on the matrix-Padé approximation) for large passive linear circuit multi-ports. The algorithm is more efficient than the more general MPVL and has the property of generating guaranteed stable and passive models for the special cases of RC, RL, and LC circuits. The algorithm is based on a novel symmetric block-Lanczos procedure.

While the reduced-order models generated by SyMPVL cannot be guaranteed to be stable and passive for general RLC circuits, they can be made stable and passive using suitable "post-processing" techniques. The will be described elsewhere.

The authors would like to thank Homer Wang for providing the package model.

References

[1] J.I. Aliaga, D.L. Boley, R.W. Freund, and V. Hernández, "A Lanczos-type algorithm for multiple starting vectors," Numerical Analysis Manuscript No. 96–18, Bell Labo-

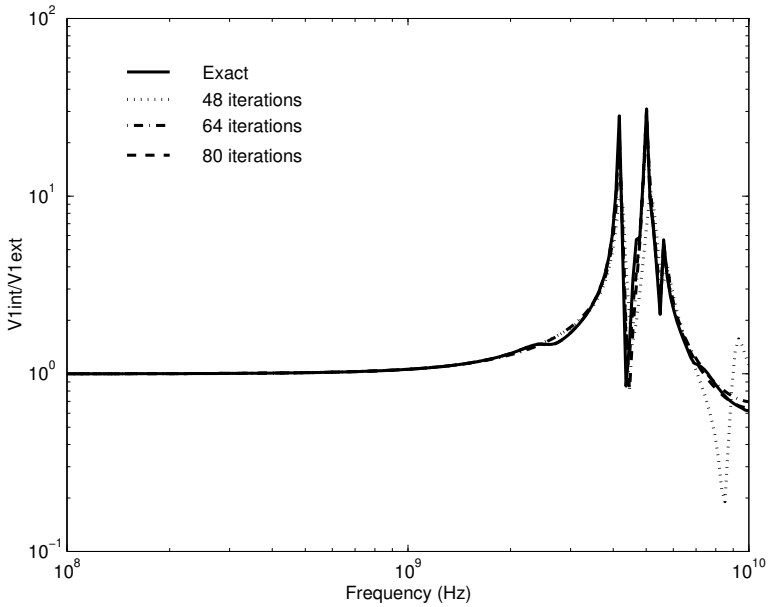

Figure 3: Package: Pin no. 1 external to Pin no. 1 internal

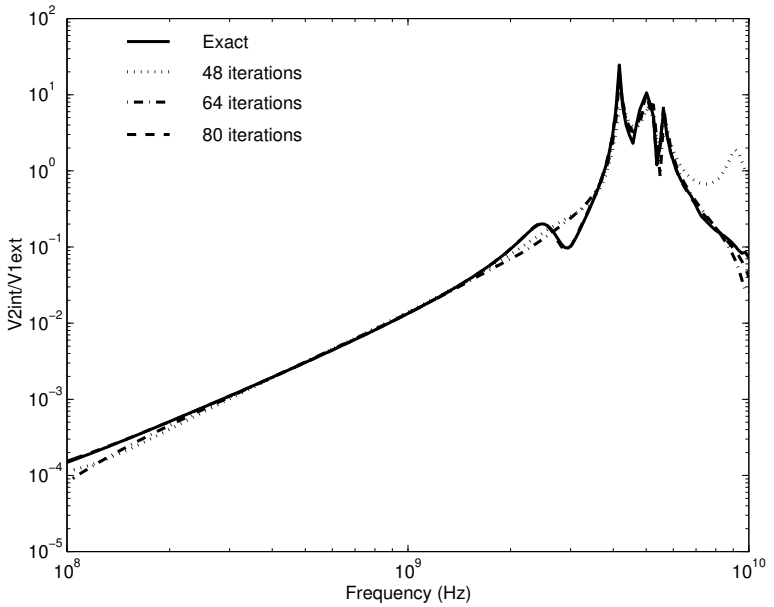

Figure 4: Package: Pin no. 1 external to Pin no. 2 internal

ratories, Murray Hill, NJ, Sep. 1996.

[2] B.D.O. Anderson and S. Vongpanitlerd, *Network Analysis and Synthesis*, Englewood Cliffs, NJ: Prentice-Hall, 1973.

[3] G.A. Baker, Jr. and P. Graves-Morris, *Padé Approximants*, Second Edition, New York, NY: Cambridge University Press, 1996.

[4] J.E. Bracken, "Algorithms for passive modeling of linear interconnect networks," manuscript.

[5] P. Feldmann and R.W. Freund, "Efficient linear circuit analysis by Padé approximation via the Lanczos process," in *Proc. Euro-DAC*, Sep. 1994.

[6] P. Feldmann and R.W. Freund, "Efficient linear circuit analysis by Padé approximation via the Lanczos process," *IEEE Trans. Computer-Aided Design*, vol. 14, pp. 639–649, May 1995.

[7] P. Feldmann and R.W. Freund, "Reduced-order modeling of large linear subcircuits via a block Lanczos algorithm," in *Proc. 32nd ACM/IEEE Design Automation Conf.*, June 1995.

[8] R.W. Freund, "An extension of the Lanczos-Padé connection to the matrix case," Numerical Analysis Manuscript, Bell Laboratories, Murray Hill, NJ, in preparation.

[9] R.W. Freund and P. Feldmann, "Reduced-order modeling of large passive linear circuits by means of the SyPVL algorithm," in *Tech. Dig. 1996 IEEE/ACM International Conference on Computer-Aided Design*, Nov. 1996.

[10] R.W. Freund and N.M. Nachtigal, "Software for simplified Lanczos and QMR algorithms," *Appl. Numer. Math.*, vol. 19, pp. 319–341, 1995.

[11] G.H. Golub and C.F. Van Loan, *Matrix Computations*, Third Edition. Baltimore, MD: The Johns Hopkins University Press, 1996.

[12] W.B. Gragg, "Matrix interpretations and applications of the continued fraction algorithm," *Rocky Mountain J. Math.*, vol. 4, pp. 213–225, 1974.

[13] K.J. Kerns and A.T. Yang, "Stable and efficient reduction of large, multiport RC networks by pole analysis via congruence transformations," manuscript.

[14] C. Lanczos, "An iteration method for the solution of the eigenvalue problem of linear differential and integral operators," *J. Res. Nat. Bur. Standards*, vol. 45, pp. 255–282, 1950.

[15] L.T. Pillage and R.A. Rohrer, "Asymptotic waveform evaluation for timing analysis," *IEEE Trans. Computer-Aided Design*, vol. 9, pp. 352–366, Apr. 1990.

[16] V. Raghavan, R.A. Rohrer, L.T. Pillage, J.Y. Lee, J.E. Bracken, and M.M. Alaybeyi, "AWE–inspired," in *Proc. IEEE Custom Integrated Circuits Conference*, May 1993.

[17] A.E. Ruehli, "Equivalent circuit models for three-dimensional multiconductor systems," *IEEE Trans. Microwave Theory and Tech.*, vol. 22, pp. 216–221, Mar. 1974.

[18] A. Ruhe, "Implementation aspects of band Lanczos algorithms for computation of eigenvalues of large sparse symmetric matrices," *Math. Comp.*, vol. 33, pp. 680–687, 1979.

[19] L.M. Silveira, M. Kamon, I. Elfadel, and J. White, "A coordinate-transformed Arnoldi algorithm for generating guaranteed stable reduced-order models of RLC circuits," in *Tech. Dig. 1996 IEEE/ACM International Conference on Computer-Aided Design*, Nov. 1996.

[20] J. Vlach and K. Singhal, *Computer Methods for Circuit Analysis and Design*, Second Edition, New York, N.Y.: Van Nostrand Reinhold, 1993.

[21] M.R. Wohlers, *Lumped and Distributed Passive Networks*, New York, N.Y.: Academic Press, 1969.